Molecules and Cells

Sub-Ciliary Segregation of Two *Drosophila* Transient Receptor Potential Channels Begins at the Initial Stage of Their Pre-Ciliary Trafficking

Youngtae Kwon[1,2], Jeongmi Lee[1,2], and Yun Doo Chung[1,*]

[1]Department of Life Sciences, University of Seoul, Seoul 02504, Korea, [2]These authors contributed equally to this work.
*Correspondence: ydchung@uos.ac.kr
https://doi.org/10.14348/molcells.2020.0205
www.molcells.org

Cilia are important eukaryotic cellular compartments required for diverse biological functions. Recent studies have revealed that protein targeting into the proper ciliary subcompartments is essential for ciliary function. In *Drosophila* chordotonal cilium, where mechano-electric transduction occurs, two transient receptor potential (TRP) superfamily ion channels, TRPV and TRPN, are restricted to the proximal and distal subcompartments, respectively. To understand the mechanisms underlying the sub-ciliary segregation of the two TRPs, we analyzed their localization under various conditions. In developing chordotonal cilia, TRPN was directly targeted to the ciliary tip from the beginning of its appearance and was retained in the distal subcompartment throughout development, whereas the ciliary localization of TRPV was considerably delayed. Lack of intraflagella transport-related proteins affected TRPV from the initial stage of its pre-ciliary trafficking, whereas it affected TRPN from the ciliary entry stage. The ectopic expression of the two TRP channels in both ciliated and non-ciliated cells revealed their intrinsic properties related to their localization. Taken together, our results suggest that sub-ciliary segregation of the two TRP channels relies on their distinct intrinsic properties, and begins at the initial stage of their pre-ciliary trafficking.

Keywords: cilia, ciliary sub-compartment, *Drosophila*, intraflagella transport, transient receptor potential channel

INTRODUCTION

The cilium, a hair-like eukaryotic cell organelle, is a distinct cellular compartment in terms of function, structure, and protein composition (Lee and Chung, 2015; Sung and Leroux, 2013). Ciliary dysfunction results in pleiotropic effects on diverse eukaryotic cells, ranging from sensory neurons to germ cells (Waters and Beales, 2011). Increasing evidence suggests that the cilia are sub-compartmentalized, and proper sub-ciliary localization of proteins is essential for their function (Lee and Chung, 2015).

Ciliary protein localization is mediated by the collaboration of two fundamentally different mechanisms: vesicular trafficking and vesicle-free trafficking, termed intraflagella transport (IFT) (Lee and Chung, 2015; Sung and Leroux, 2013). The first stage of ciliary trafficking, pre-ciliary trafficking, relies on the canonical vesicular trafficking pathway, which is initiated by sorting in the trans-Golgi network. Coat assembly mediated by coat proteins produces cilium-destined vesicles; these vesicles are targeted to the periciliary membrane (PCM) near the ciliary base region. At least three different trafficking routes have been proposed that can be used by vesicles to reach the PCM: direct targeting to the PCM, recycling endosome-mediated targeting to the PCM, and lateral diffusion to the PCM after targeting the nearby apical membrane (Sung and Leroux, 2013). After reaching the PCM, cilium-destined proteins must be re-sorted and loaded onto the IFT trains at

Received 19 October, 2020; revised 15 November, 2020; accepted 15 November, 2020; published online 15 December, 2020

eISSN: 0219-1032

the PCM. The BBSome, which is a stable complex of proteins associated with a ciliopathy called the Bardet–Biedl syndrome (BBS), is believed to be the authentic sorting machinery for ciliary targeting (Jin et al., 2010). In addition to the three pathways mentioned above, another pathway independent of the BBSome has also been reported. In this pathway, UNC119, which is a GTP-specific interacting protein of the small GTPase ARL3, binds to a subset of myristoylated proteins and plays a central role in their ciliary targeting (Wright et al., 2011).

After passing the transition zone (TZ), which is the selective gate located at the base of the cilium, most cargo proteins rely on IFT particles for their intra-ciliary trafficking. IFT particles are motor-associated multi-protein complexes that can be categorized into two sub-complexes, IFT-A and IFT-B (Taschner and Lorentzen, 2016). The associated motor proteins, kinesin-II and cytoplasmic dynein 2, transport the cargo-laden IFT particles from the ciliary base to the tip and in the opposite direction, respectively. Although there is significant information regarding the mechanism underlying the intra-ciliary trafficking in general (Morthorst et al., 2018), the mechanism by which the IFT segregates some proteins into distinct ciliary subcompartments remains unclear.

Drosophila chordotonal neurons, which act as stretch receptors, are an effective model to study the mechanism underlying sub-ciliary protein segregation. The dendrites of chordotonal neurons can be divided into two structurally distinct segments, i.e., inner and outer segments, in which the latter is a ciliary compartment. The chordotonal cilium can be further divided into the following distinct subcompartments: the TZ, the proximal subcompartment, the ciliary dilation (CD), and the distal subcompartment (Lee and Chung, 2015). CD, which is a bulging region in the middle of the cilium, separates the compartment into the proximal and distal subcompartments (Lee and Chung, 2015). Two TRP channels, TRPV and TRPN, are essential for the mechano-electric transduction and amplification in chordotonal neurons (Gong et al., 2004; Gopfert et al., 2006; Kim et al., 2003; Lehnert et al., 2013; Walker et al., 2000; Yan et al., 2012). TRPV comprises two different subunits encoded by *inactive* (*iav*) and *nanchung* (*nan*), whereas *no mechanoreceptor potential C* (*nompC*) encodes TRPN (Gong et al., 2004; Kim et al., 2003; Walker et al., 2000). Interestingly, they are localized in distinct subcompartments of chordotonal cilia; TRPV is in the proximal subcompartment, whereas TRPN is in the distal subcompartment (Lee et al., 2010). Although the loss of several IFT-related proteins affects their localization, the mechanism by which the two TRPs are segregated in the same cellular compartment requires elucidation. Here, we analyzed the localizations of two TRPs under various conditions and found that their segregation was mediated by two distinct pathways from the beginning of their route to the cilium.

MATERIALS AND METHODS

Fly stocks

Flies were cultured on standard media at 25°C. The following mutant alleles for IFT-related proteins were used: btv^{5p1} (Eberl et al., 2000), $rempA^{1}$ (Lee et al., 2008), and $dTulp^{1}$ (Park et al., 2013). The *UAS-nan* (Kim et al., 2003) and the GFP-tagged IAV (IAV::eGFP) (Gong et al., 2004) lines used in the study have been described earlier. The pan-neuronal *elav*-GAL4 (*P{GawB}elav*^{C155}; BL#458) and the salivary gland GAL4 (AB1-GAL4; BL#1824) lines were obtained from the Bloomington Drosophila Stock Center and were used to induce TRP channel expression in olfactory neurons and salivary gland cells, respectively. A *nompA*-GAL4 driver (this study) was used to induce TRP channel expression in scolopale cells. The following DNA constructs were generated to produce transgenic fly lines. For the *UAS-iav::eGFP* line, the 5′ region of the GFP-tagged IAV genomic construct (*iav::eGFP*) was replaced with a 478-bp cDNA fragment of *iav* (from the 5′ end to the *SacII* site of the second exon) to generate a cDNA/genomic fusion construct and was cloned into the pUAST vector. To generate the *nompA-GAL4* line, a 1.5-kbp *BamHI/PstI* restriction fragment of the *nompA* upstream region was cloned into the pPTGAL vector (Sharma et al., 2002). The *UAS-nompC::tdTomato* construct was generated by inserting a *tdTomato* ORF near the end of exon 18 and was cloned into a modified pUAST vector containing the *attB* integration site. The *UAS-iav::eGFP* and *nompA-GAL4* transgenic lines were generated via P-element-mediated germline transformation. The *UAS-nompC::tdTomato* transgenic line was generated using the PhiC31 integrase system using VK00001 as the landing site (Venken et al., 2006).

Flies with the following genotypes were generated and used in this study: w^{1118}*; P{iav::eGFP}* (Fig. 1), w^{1118}*;* btv^{5p1}*; P{iav::eGFP}* (Fig. 2A), w^{1118}*;* $rempA^{1}$*; P{iav::eGFP}* (Fig. 2B), w^{1118}*;* $dTulp^{1}$*; P{iav::eGFP}* (Fig. 2C), *P{GawB}elav*^{C155}*; P{UAS-iav::eGFP} P{UAS-nompC::tdTomato}/SM6B* (Fig. 3A), *P{GawB}elav*^{C155}*; P{UAS-iav::eGFP} P{UAS-nan}/P{UAS-nompC::tdTomato}* (Fig. 3B), *P{GawB}elav*^{C155}*; P{UAS-iav::eGFP} P{UAS-nan}* $dTulp^{1}$*/P{UAS-nompC::tdTomato}* $dTulp^{1}$ (Fig. 3C), *P{GawB}AB1; P{UAS-iav::eGFP}* (Fig. 4A), *P{GawB}AB1; P{UAS-iav::eGFP} P{UAS-nan}/SM6b* (Fig. 4B), *P{GawB}AB1; P{UAS-nompC::tdTomato}* (Figs. 4C and 4D), *P{nompA-PTGAL}; P{UAS-iav::eGFP}* (Fig. 4E), *P{nompA-PTGAL}; P{UAS-iav::eGFP} P{UAS-nan}/SM6b* (Fig. 4F), and *P{nompA-PTGAL}; P{UAS-nompC::tdTomato}* (Fig. 4G).

Antibodies

The following antibodies were used in this study: guinea pig anti-NOMPC (TRPN) antiserum (this study, 1:1,000-1:3,000 dilution), chicken anti-GFP polyclonal antibody (#PA1-9533, 1:500 dilution; Invitrogen, USA), rabbit anti-NOMPA antiserum (1:1,500 dilution; Chung et al., 2001), rabbit anti-horseradish peroxidase (HRP) (#P7899, 1:1,000 dilution; Sigma-Aldrich, USA), and mAb 22C10 (1:100 dilution; DSHB, USA). All secondary antibodies were purchased from Thermo Fisher Scientific (USA) and used at the dilutions indicated: Alexa-488-conjugated goat anti-chicken IgY (#A11039, 1:500), Alexa-546-conjugated goat anti-guinea pig IgG (#A11074, 1:500), Alexa-633-conjugated goat anti-mouse IgG (#A21050, 1:500), and Alexa-633-conjugated goat anti-rabbit IgG (#A21071, 1:500). Alexa-633-conjugated phalloidin (#A22284; Thermo Fisher Scientific) was used to visualize the scolopale rods. Hoechst 33258 (#861405; Sigma-Aldrich) was used to stain DNA.

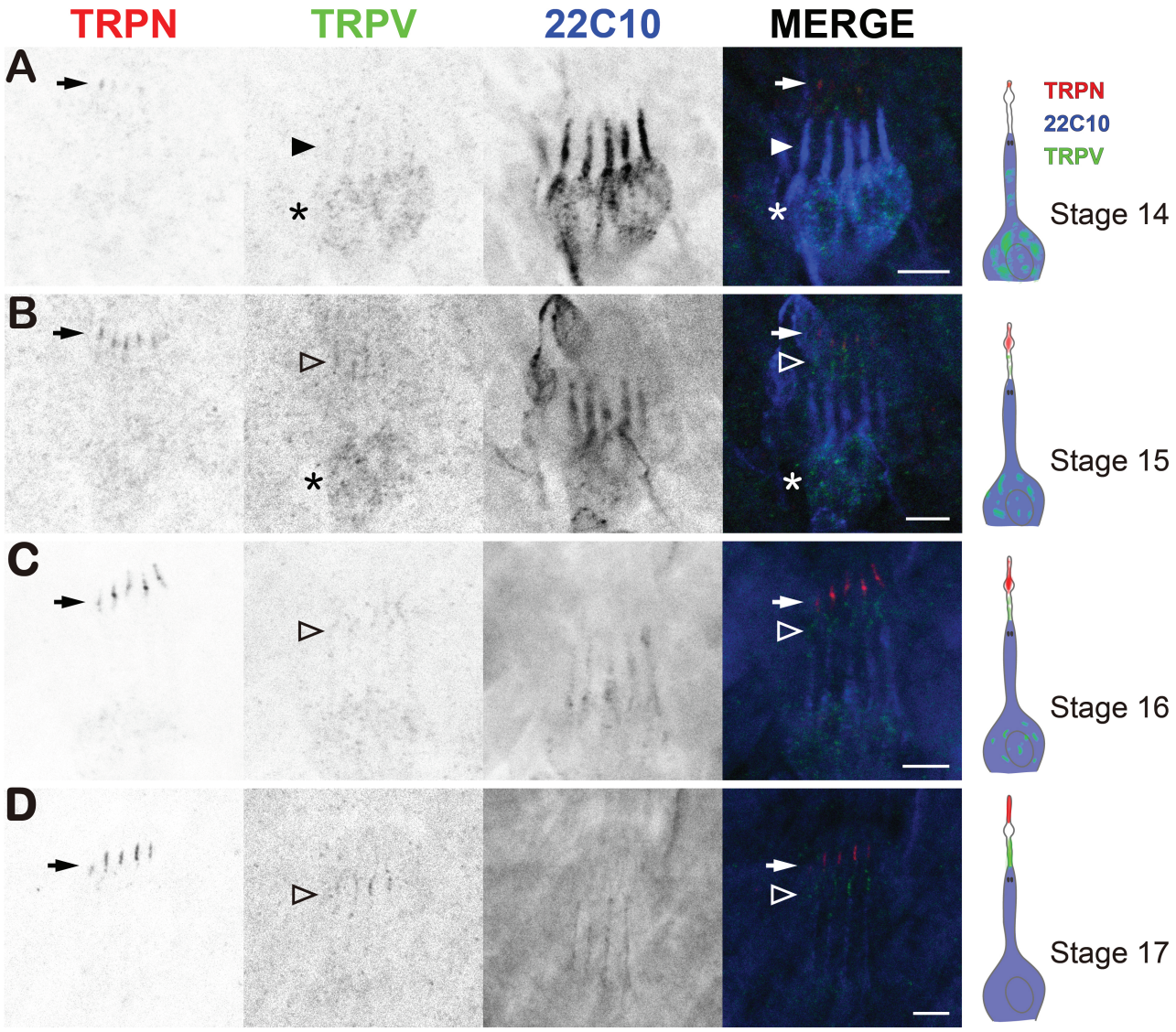

Fig. 1. Localization of TRP channels in the developing chordotonal neurons. Embryonic chordotonal neurons were labeled with an anti-NOMPC antibody (red) and IAV::eGFP (green) to reveal the localization of TRPN and TRPV, respectively. The mAb 22C10 (blue) was used to label the neuronal membrane, except for the ciliary compartment. (A) Embryonic stage 14. TRPN is enriched at the distal tip (arrows). The TRPN-enriched region is far distal to the inner dendritic segment (closed arrowheads), which suggests that it is near the ciliary tip. In contrast, TRPV signals are mostly detected in the cell body (asterisks). (B) Embryonic stage 15. TRPN-enriched signals are much more elongated (arrows). TRPV is also detectable in the cilia, but only in the proximal region (open arrowheads), although a significant amount of signal can be observed in the cell body (asterisks). (C and D) In the later embryonic stages, both TRPs are mainly detected in the cilia. Their sub-ciliary localization does not overlap throughout development, retaining TRPN in the distal (arrows) and TRPV (open arrowheads) in the proximal regions. Scale bars = 5 μm.

Immunostaining and confocal microscopy

For whole-mount embryo staining, flies were allowed to lay eggs on apple juice-agar plates for 24 h at room temperature. Embryos were collected, de-chorionated, fixed, and stained according to the standard method (Patel, 1994). The anti-GFP chicken IgY was used to enhance the IAV::eGFP signals. Neurons were visualized using an anti-HRP antibody or mAb 22C10. TRPN was detected using an anti-NOMPC guinea pig antiserum. After staining with these antibodies followed by incubation with the appropriate secondary antibodies, embryos were mounted using mountain solution (80% glycerol). For whole-mount antennal staining, pupal antennae were prepared and stained as described previously (Lee et al., 2010). For staining of salivary glands, wondering stage larvae were collected and dissected to obtain salivary glands. The tissues were fixed in 4% paraformaldehyde in phosphate-buffered saline with Triton (PBST) (10 mM $NaPO_4$ [pH 7.2], 150 mM NaCl, 0.3% Triton X-100) for 10 min,

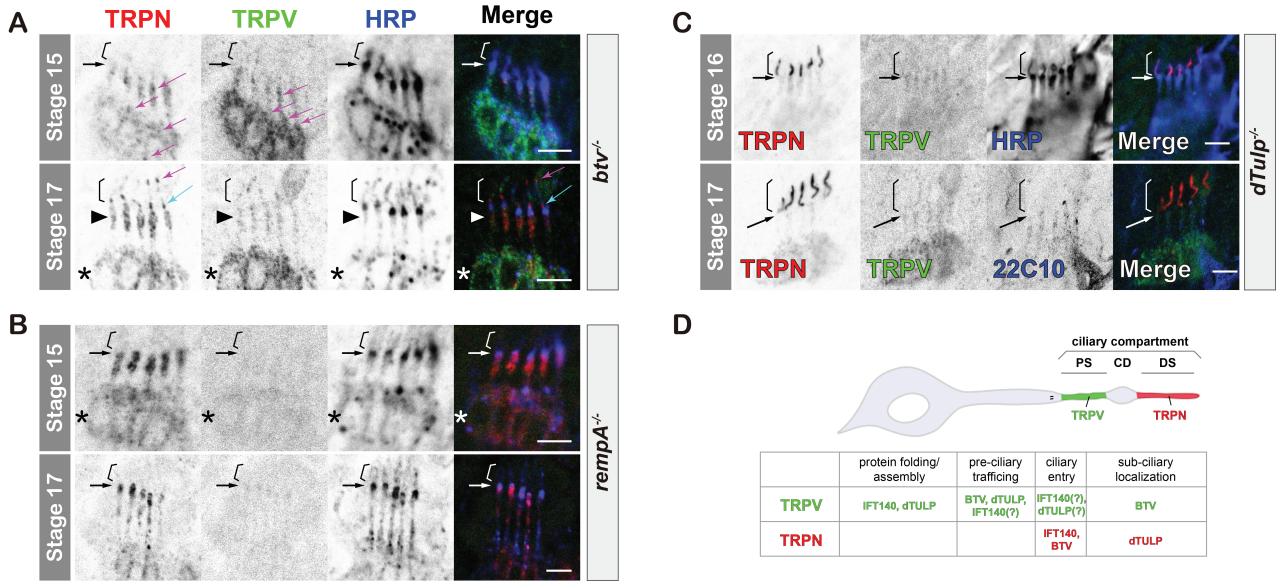

	protein folding/ assembly	pre-ciliary trafficing	ciliary entry	sub-ciliary localization
TRPV	IFT140, dTULP	BTV, dTULP, IFT140(?)	IFT140(?), dTULP(?)	BTV
TRPN			IFT140, BTV	dTULP

Fig. 2. Differential effects of IFT-related proteins on the ciliary localizations of TRPs. TRPN (red) and TRPV (green) were labeled as described in Fig. 1. Neurons were counter-stained (blue) with anti-HRP or mAb 22C10. (A) TRP localization in *btv* embryo. At stage 15, both channels were not detected in the cilia (brackets). Arrows indicate the basal body region. Several vesicle-like dots of both channels were observed in the cell body and inner dendritic segments (magenta arrows). At stage 17, few signals are detected in the cilia (brackets), although extra-ciliary signals are markedly stronger. In the cilia, TRPN is enriched in the distal tip (magenta arrows) as well as near the base (cyan arrows). The extra-ciliary TRPN signal is evidently stronger in the inner dendritic segments (arrowheads), compared with that in the cell bodies (asterisks), whereas the opposite is true in the case of TRPV. (B) TRP localization in *rempA* embryo. Both channels never reach the cilia (brackets). TRPN is accumulated just below the cilia (arrows) with weak signals in the cell body region (asterisks), whereas TRPV is almost undetectable. (C) TRP localization in *dTulp* embryo. TRPN is enriched in the cilium from its base (arrows) up to its distal end (brackets), whereas no ciliary signal of TRPV is observed. Scale bars = 5 μm. (D) Summary of roles of IFT-related proteins on TRP channel localization. In each trafficking step, the two TRPs require different sets of proteins. PS, proximal segment; CD, ciliary dilation; DS, distal segment.

and then washed three times in PBST for 10 min each. After blocking for 1 h in blocking solution (2% normal goat serum, 2% BSA in PBS), the tissues were incubated with primary antibodies overnight at 4°C. After three 10-min washes with PBST, the tissues were incubated with the appropriate secondary antibodies for 1 to 2 h at room temperature. Next, after another three 10-min washes with PBST, the tissues were mounted in 80% glycerol. All images were obtained using a laser scanning confocal microscope (LSM510; Carl Zeiss, Germany).

RESULTS

The two TRP channels use distinct routes for their ciliary localization from the initial stage of trafficking

To analyze TRP channel trafficking, we examined their localization in the lateral chordotonal organs (lch5) of developing embryos. During embryogenesis, the chordotonal organs start differentiating at stage 13 and are fully differentiated by the end of stage 17 (Hartenstein, 1988). Confocal imaging of endogenous TRPN and a functional GFP-tagged TRPV driven by the endogenous promoter showed that the channels could first be detected in stage 14 embryos (Fig. 1). At this stage, TRPV was mainly detected in the cell body, although some faint signals of apically transported TRPV were detected in the inner dendritic segment (Fig. 1A). In the later stage embryos (stage 15-16), however, the apically transported TRPV was now mainly localized in the proximal cilium, although the cell body signal remained prominent (Fig. 1B). The ciliary localization of TRPV became more evident as the embryo developed and was almost exclusively restricted in the proximal region at the final stage of embryonic development (Figs. 1C and 1D).

Unlike TRPV, TRPN was enriched in the distal region of developing cilia from the beginning of its appearance, (Fig. 1A). Co-staining with anti-HRP antibody, which labels the entire neuronal boundary including the ciliary outer dendritic segment, revealed that the TRPN-enriched region corresponded to the ciliary tip (Supplementary Fig. S1A). This result was further confirmed by co-labeling with No mechanoreceptor potential A (NOMPA), which is a dendrite cap protein (Supplementary Fig. S1B). In chordotonal organs, NOMPA is known to be expressed by the scolopale cell that ensheathes sensory neurons and is transported to the apical tip, followed by secretion into the extracellular space to form the dendrite cap, which covers the distal end of the sensory cilia (Chung et al., 2001; Lee et al., 2010). In the developing chordotonal organ, the TRPN-enriched region overlapped with the end of

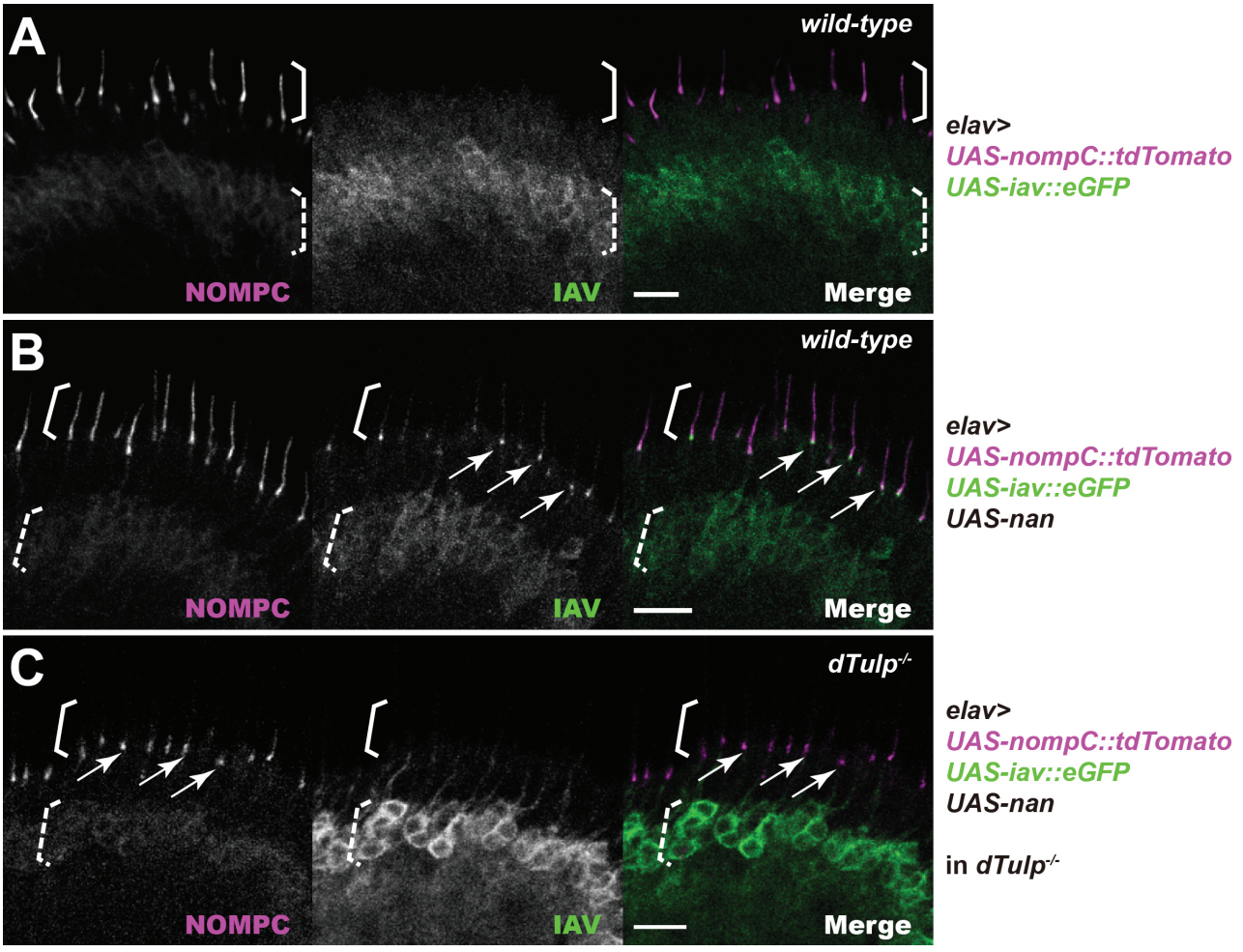

Fig. 3. Ectopic expression of TRP channels in the ciliated cells. Olfactory neurons of antennal trichoid sensilla. NOMPC::tdTomato (magenta) and IAV::eGFP (green) were ectopically expressed using a pan-neuronal GAL4 driver. NOMPC::tdTomato is enriched in the cilia (brackets) from their base to their distal end. However, without NAN, IAV::eGFP is retained in the cell body (dotted brackets) (A). Co-expression of NAN drives IAV::eGFP to the cilia, mostly to the basal region (arrows) (B). In *dTulp* mutant (C), TRPV (green) is not detected in the ciliary region (brackets), rather it is enriched in the cell body region (dotted brackets). TRPN (magenta) is enriched in the proximal ciliary region (arrows) but not in the distal region. Scale bars = 5 μm.

the scolopale cell where NOMPA was accumulated, revealing that TRPN was localized at the distal end of the cilium (Supplementary Fig. S1B).

Taken together, our results suggest that TRPN possesses the intrinsic property to be targeted to the ciliary distal subcompartment as soon as it is produced, whereas TRPV may need prerequisites for its ciliary entry and trafficking. In the ciliary compartment, TRPV localization never proceeds beyond the proximal subcompartment, whereas TRPN is retained mostly in the distal subcompartment throughout development.

Two TRPs require IFT proteins at different stages of their targeting to the ciliary compartment

Previous studies have reported that several IFT-related proteins are required for the proper localization of both TRPs in the antennal auditory organ, termed Johnston's organ (JO) (Lee et al., 2008; 2010; Park et al., 2013). However, it was difficult to analyze their precise roles because JO is a complicated organ comprising hundreds of chordotonal sensilla, each of which possesses two or three sensory neurons. Thus, we examined the lch5 of developing embryos, which contains only five sensilla each with a single neuron, to comprehensively analyze the defects caused by IFT-related protein dysfunction. We first analyzed embryos lacking Beethoven (BTV), which is a subunit of cytoplasmic dynein that acts as a retrograde motor for IFT (Eberl et al., 2000). In all stages of mutant embryos, both TRPs were mainly detected outside the cilia, suggesting that pre-ciliary trafficking or ciliary entry might require BTV (Fig. 2A). Interestingly, the accumulation of TRPN, but not TRPV, was evident near both sides of the ciliary base region in late embryos, suggesting that TRPN required BTV mainly for ciliary entry rather than pre-ciliary apical trafficking, whereas the opposite is true for TRPV (Fig. 2A).

Although apical trafficking or ciliary entry of both TRPs was defective, faint signals could be detected in the cilia. Upon entering the ciliary compartment, TRPN was preferentially targeted to the distal tip, whereas TRPV was unevenly distributed throughout the cilium (Fig. 2A). This finding further supported the intrinsic property of TRPN, which drives itself to the distal end of the cilium. In contrast, retaining TRPV in the proper sub-ciliary region might require BTV or a normal ciliary structure.

We next analyzed a *Drosophila* IFT-A component, IFT140, which is encoded by *reduced mechanoreceptor potential A* (*rempA*). Consistent with the results of a previous report in JO (Lee et al., 2008), TRPV was almost undetectable even in the cell body of the mutant embryonic chordotonal neurons (Fig. 2B). Interestingly, the faint cell body signal of TRPV weakened at the late stage, suggesting that IFT140 might be necessary to assemble the transport-competent TRPV at the initial sorting stage, and failure of this process might affect its stability (Fig. 2B). Unlike TRPV, strong TRPN signals were detected outside the cilium, especially in the inner dendritic segment of *rempA* (Fig. 2B). Interestingly, the accumulation of TRPN in the distal region of the inner dendritic segment was evident in late-stage mutant embryos, suggesting that the pre-ciliary apical trafficking of TRPN was considerably unaffected by the loss of IFT-A function (Fig. 2B). However, no sign of TRPN was observed in the cilia, suggesting that its ciliary entry required IFT-A or normal ciliary structure (Fig. 2B).

The mammalian Tubby family proteins, Tubby (TUB) and Tubby-like protein 3 (TULP3), are implicated in the ciliary trafficking of many membrane proteins, including several GPCRs, fibrocystin, and polycystin 2 (PC2) (Morthorst et al., 2018). A similar role for a *Drosophila* Tubby protein, dTULP,

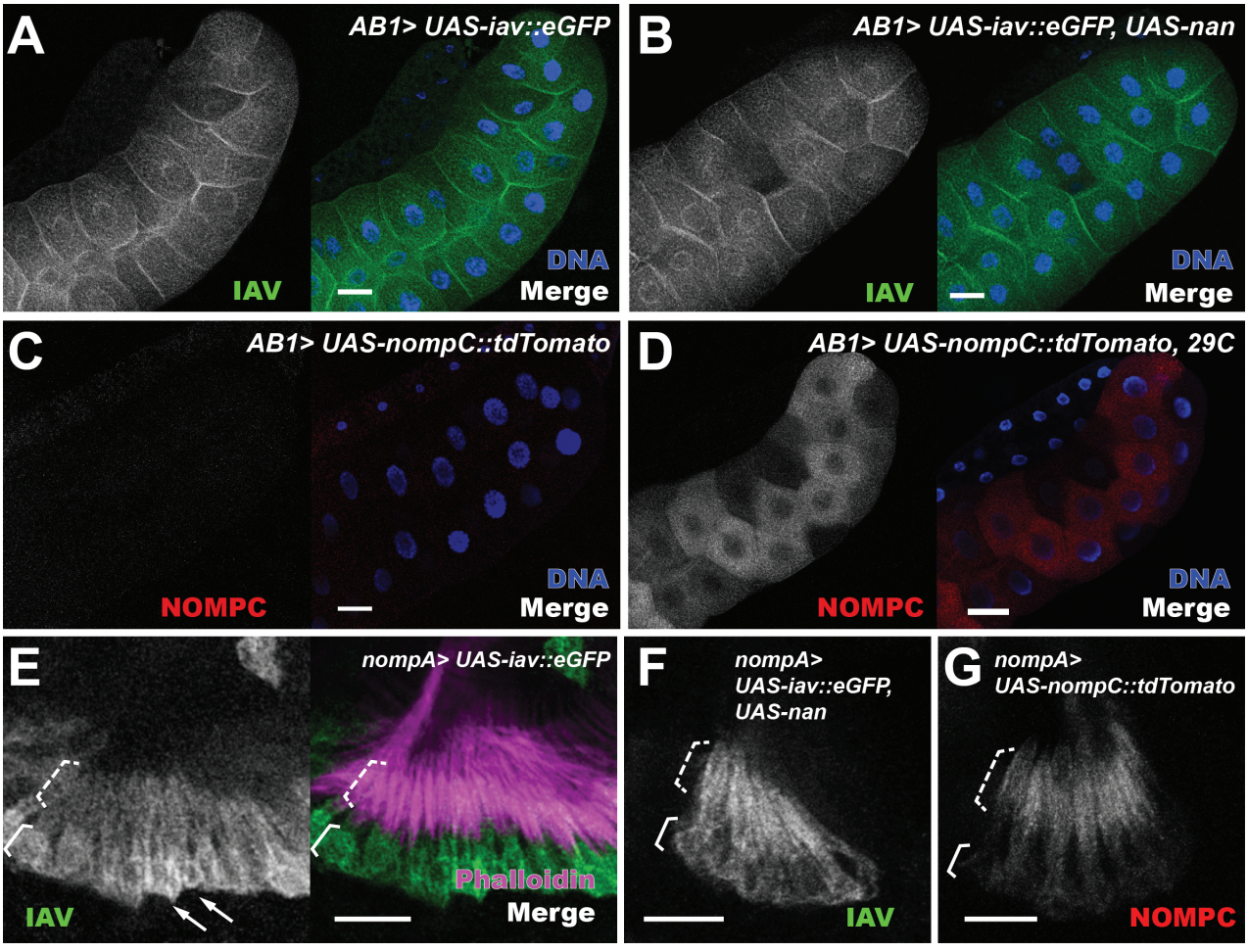

Fig. 4. Ectopic expression of TRP channels in the non-ciliated cells. NOMPC::tdTomato (magenta) and IAV::eGFP (green) were ectopically expressed using appropriate GAL4 drivers. (A-D) Salivary gland cells. Hoechst 33258 (blue) was used to visualize the nucleus. IAV::eGFP, either alone (A) or with NAN (B), is localized in the membranes, whereas NOMPC::tdTomato is de-localized (C and D). NOMPC::tdTomato is undetectable under usual induction condition (25°C) (C). By increasing GAL4 activity (29°C), de-localized NOMPC::tdTomato signals can be seen (D). (E-G) Scolopale cells of JO. Phalloidin (magenta) was used to stain actin-packed scolopale rods in the distal part of the cell (E). IAV::eGFP alone is mainly located in the basolateral membrane (arrows) surrounding the cell body (brackets) (E). When co-expressed with NAN, IAV::eGFP is preferentially detected in the apical membrane (dotted brackets) (F). NOMPC::tdTomato is mainly detected in the apical membrane (G). Scale bars = 50 μm (A-D), 10 μm (E-G).

has also been reported. When dTULP is defective in JO, ciliary localization of TRPV is completely abolished, whereas TRPN is abnormally enriched in the proximal subcompartment (Park et al., 2013). In the *dTulp* mutant embryos, we found similar defects (Fig. 2C). Interestingly, some vesicle-like speckles of TRPV were detected in the cell body of later embryonic chordotonal neurons, suggesting that dTULP was required for its apical trafficking (Fig. 2C). The altered localization of TRPN caused by the loss of dTULP in the lch5 was also comparable to that in the JO. The TRPN-localized ciliary region was elongated from the distal tip down to the ciliary base, suggesting that dTULP was required to establish the integrity of the proximal subcompartment or for the sub-ciliary trafficking of TRPN (Fig. 2C).

In summary, the results showed that the pre-ciliary trafficking of TRPV, but not of TRPN, was consistently affected by all three IFT-related proteins, suggesting that TRPV required IFT proteins from the initial stage of its trafficking, whereas the pre-ciliary trafficking of TRPN relied on an IFT-independent pathway. These results also showed that IFT proteins participated in the localization of TRPN only after the pre-ciliary trafficking stage (Fig. 2D).

Ectopic expression of TRP channels in ciliated cells reveals their intrinsic properties for the sub-ciliary localization

If both TRPs possess distinct intrinsic properties in terms of sub-ciliary localization, their ectopic expression in other types of ciliated cells should also demonstrate a segregated localization pattern. To test this hypothesis, we ectopically expressed the fluorescently tagged TRP channels in the olfactory neurons, which have a much simpler sub-ciliary structure with no CD, and then analyzed their localization. When a GFP-tagged subunit of TRPV (IAV::eGFP) alone was induced in the olfactory neurons via a pan-neuronal *elav*-GAL4 driver, most GFP signals were observed in the membrane surrounding the cell body (Fig. 3A). However, co-expression of NAN facilitated the re-localization of IAV::GFP mainly to the proximal base of the cilia (Fig. 3B), reminiscing the subunit inter-dependency of TRPV in JO (Gong et al., 2004; Supplementary Figs. S2A and S2B). Meanwhile, most ectopically expressed TRPN (NOMPC::tdTomato) were found in the cilia, indicating that TRPN harbored an intrinsic signal for ciliary targeting (Figs. 3A and 3B). Interestingly, the sub-ciliary distribution of NOMPC::tdTomato was also reminiscent of that in chordotonal cilia; NOMPC::tdTomato partially co-localized with IAV::GFP in the proximal region but was evenly localized up to the distal cilia (Figs. 3A and 3B). However, NOMPC::tdTomato failed to be targeted to the distal cilia when dTULP was deficient, suggesting dTULP was an authentic key player for the sub-ciliary trafficking of TRPN (Fig. 3C).

In summary, these results imply that both TRPs exhibit intrinsic preferences for their sub-ciliary localization, regardless of the sub-ciliary structure. As the fluorescently tagged TRP channels used in this study demonstrated the same pattern of sub-ciliary segregation in JO as the endogenous proteins (Supplementary Fig. S2C), their localization properties in the olfactory neurons were not attributed to the artificial effect of the fluorescent tags. Our results also suggested that dTULP, rather than sub-ciliary compartmentalization *per se*, was important for the sub-ciliary segregation of the two TRP channels, especially for the targeting of TRPN into the distal cilia.

Ectopic expression of TRP channels in non-ciliated cells reveals their intrinsic properties for the pre-ciliary trafficking

If TRPN and TRPV rely on distinct pre-ciliary trafficking pathways, their distributions should also be different in non-ciliated cells. To test this hypothesis, we ectopically expressed TRPN and TRPV in salivary gland cells. Unlike the case in ciliated cells, the localization profile of IAV::eGFP was not affected by NAN. With or without NAN, IAV::GFP signals labeled the outlines of the cell and its nucleus, suggesting that it was targeted to most types of cellular membranes (Figs. 4A and 4B). In contrast, the ectopically expressed NOMPC::tdTomato was completely delocalized (Figs. 4C and 4D). This suggested that the sorting mechanism that targeted TRPN to the membrane was cell type-specific.

As salivary gland cells are non-polarized cells, it is unclear whether both channels possess intrinsic properties for apical trafficking in non-ciliated cells. To explore this further, we expressed both channels in polarized cells, the scolopale cells. When expressed alone, IAV::eGFP preferentially targeted the basolateral membrane (Fig. 4E). However, co-expression with NAN significantly relocated IAV::eGFP into the apical membrane (Fig. 4F), suggesting that IAV alone had an intrinsic membrane-targeting property but required NAN for apical trafficking in polarized cells. In the case of TRPN, unlike in non-polarized cells, it was not only targeted to the membrane but was also efficiently localized to the apical membrane, showing its intrinsic apical trafficking property in polarized cells (Fig. 4G).

Taken together, the ectopic expression studies in non-ciliated cells implied that IAV alone had an intrinsic membrane-targeting property that was mediated by the general membrane trafficking pathway; however, presence of NAN is vital for targeting the apical membrane in polarized cells. In contrast, membrane targeting of TRPN is polarized cell-specific, and an apical trafficking machinery is required for membrane targeting of TRPN.

DISCUSSION

Here, we analyzed the ciliary localization of two *Drosophila* TRPs and found that they utilized distinct pathways from the initial stage of their trafficking. In developing chordotonal neurons, ciliary targeting of TRPV was delayed compared with that of TRPN. The delay could be due to the delayed establishment of subcompartmental integrity, especially in the proximal subcompartment. Alternatively, the trafficking route of TRPV may involve multiple steps, such as the recycling endosome-mediated route, which requires re-sorting at the recycling endosome for targeting to the PCM. It cannot be ruled out that the expression of factor(s), such as IFT proteins, necessary for the ciliary targeting of TRPV may be delayed.

By using developing embryos, the roles of some IFT-related proteins in TRP localization have been clarified. From the initial protein assembly to the final sub-ciliary localization stages, distinct sets of these proteins were involved in TRP localization (Fig. 2D). Particularly, defects caused by a lack of BTV

were more clearly observed than the results previously reported in the JO (Lee et al., 2010). In the ciliary compartment, TRPN was bipartitely localized to the distal end and the basal end near the TZ (Fig. 2A). This result suggests that BTV may be involved in the retrograde movement of TRPN in the ciliary distal subcompartment, but not in the proximal subcompartment. Consistent with this finding, a recent time-lapse live-cell imaging study has shown that the velocity of retrograde movement of the IFT in the chordotonal neurons of the JO differs between the proximal and distal subcompartments, suggesting that distinct retrograde movement mechanisms are involved in the two subcompartments (Lee et al., 2018).

Another important finding is that all IFT proteins examined in this study consistently affected pre-ciliary apical trafficking of TRPV but not that of TRPN. These results suggest that the pre-ciliary trafficking pathway of TRPV may rely on the IFT-dependent pathway, such as the direct targeting pathway. In the direct targeting pathway to the PCM, a small GTPase, Arf4, regulates the budding of coated vesicles that harbor cilium-destined membrane proteins (Mazelova et al., 2009). During the route to the PCM, IFT proteins may also ride on the vesicle (Follit et al., 2006). Cargo proteins in this route usually contain a cytoplasmic ciliary targeting signal, called the VxPx motif, which interacts with regulatory proteins, such as Arf4 (Mazelova et al., 2009). However, we failed to detect the VxPx motif in either IAV or NAN subunit of TRPV. Thus, the involvement of other pathways such as the recycling endosome-mediated route discussed above cannot be ruled out.

Finally, the ectopic expression studies revealed the distinct intrinsic properties of the two TRPs regarding their localization. IAV alone had an intrinsic membrane-targeting property; however, NAN was required for trafficking to the apical membrane. In contrast, membrane targeting of TRPN was polarized cell-specific, and membrane-destined TRPN showed intrinsic preference for apical trafficking. Interestingly, the apical trafficking of TRPN was much more evident than that of TRPV (IAV + NAN) in polarized cells (compare Figs. 4F and 4G), suggesting that the apical trafficking of TRPV was inefficient in non-ciliated cells. This result further supported the idea that the pre-ciliary trafficking of TRPV, but not TRPN, requires IFT proteins. Additionally, the finding that preferential localization of ectopically expressed TRPN into the distal cilia, which is compromised by lack of dTULP, provided an important clue for understanding the mechanism of TRPN targeting to the distal cilia. As the olfactory cilia do not possess a CD that separates the ciliary compartment into distinct subcompartments, targeting of TRPN into the distal cilia relies on specific trafficking factor(s) such as dTULP, rather than sequestration or tethering by a specific structure. Although, our present study provides novel evidence to broaden our understanding of sub-ciliary localization of two TRP channels, further studies using mutant flies lacking other IFT or trafficking-related proteins will enable us to better understand their trafficking and sub-ciliary segregation.

Note: Supplementary information is available on the Molecules and Cells website (www.molcells.org).

ACKNOWLEDGMENTS

We thank Maurice Kernan (Stony Brook University, USA) for *rempA*^{1} and *btv*^{p51} fly stocks and supporting to generate some transgenic lines. We also thank Bloomington Stock Center, and the Developmental Studies Hybridoma Bank for the fly stocks and monoclonal antibodies. This work was supported by a National Research Foundation of Korea (NRF) grant funded by the Korean government (MSIT) (2018R1A2A2A05023592), and the 2018 sabbatical year research grant of the University of Seoul to Y.D.C.

AUTHOR CONTRIBUTIONS

Y.K. performed the analyses in embryos. The ectopic expression studies were performed by J.L. Transgenic fly lines were generated by J.L. and Y.D.C. The writing of the manuscript and funding acquisition were done by Y.D.C.

CONFLICT OF INTEREST

The authors have no potential conflicts of interest to disclose.

ORCID

Youngtae Kwon https://orcid.org/0000-0001-8944-0704
Jeongmi Lee https://orcid.org/0000-0002-9470-656X
Yun Doo Chung https://orcid.org/0000-0002-6041-1472

REFERENCES

Chung, Y.D., Zhu, J., Han, Y., and Kernan, M.J. (2001). *nompA* encodes a PNS-specific, ZP domain protein required to connect mechanosensory dendrites to sensory structures. Neuron *29*, 415-428.

Eberl, D.F., Hardy, R.W., and Kernan, M.J. (2000). Genetically similar transduction mechanisms for touch and hearing in *Drosophila*. J. Neurosci. *20*, 5981-5988.

Follit, J.A., Tuft, R.A., Fogarty, K.E., and Pazour, G.J. (2006). The intraflagellar transport protein IFT20 is associated with the Golgi complex and is required for cilia assembly. Mol. Biol. Cell *17*, 3781-3792.

Gong, Z., Son, W., Chung, Y.D., Kim, J., Shin, D.W., McClung, C.A., Lee, Y., Lee, H., Chang, D.J., Kaang, B.K., et al. (2004). Two interdependent TRPV channel subunits, Inactive and Nanchung, mediate hearing in *Drosophila*. J. Neurosci. *24*, 9059-9066.

Gopfert, M.C., Albert, J.T., Nadrowski, B., and Kamikouchi, A. (2006). Specification of auditory sensitivity by *Drosophila* TRP channels. Nat. Neurosci. *9*, 999-1000.

Hartenstein, V. (1988). Development of *Drosophila* larval sensory organs: spatiotemporal pattern of sensory neurones, peripheral axonal pathways and sensilla differentiation. Development *102*, 869-886.

Jin, H., White, S.R., Shida, T., Schulz, S., Aguiar, M., Gygi, S.P., Bazan, J.F., and Nachury, M.V. (2010). The conserved Bardet-Biedl syndrome proteins assemble a coat that traffics membrane proteins to cilia. Cell *141*, 1208-1219.

Kim, J., Chung, Y.D., Park, D.Y., Choi, S., Shin, D.W., Soh, H., Lee, H.W., Son, W., Yim, J., Park, C.S., et al. (2003). A TRPV family ion channel required for hearing in *Drosophila*. Nature *424*, 81-84.

Lee, E., Sivan-Loukianova, E., Eberl, D.F., and Kernan, M.J. (2008). An IFT-A protein is required to delimit functionally distinct zones in mechanosensory cilia. Curr. Biol. *18*, 1899-1906.

Lee, J. and Chung, Y.D. (2015). Ciliary subcompartments: how are they established and what are their functions? BMB Rep. *48*, 380-387.

Lee, J., Moon, S., Cha, Y., and Chung, Y.D. (2010). *Drosophila* TRPN (= NOMPC) channel localizes to the distal end of mechanosensory cilia. PLoS

One *5*, e11012.

Lee, N., Park, J., Bae, Y.C., Lee, J.H., Kim, C.H., and Moon, S.J. (2018). Time-lapse live-cell imaging reveals dual function of Oseg4, *Drosophila* WDR35, in ciliary protein trafficking. Mol. Cells *41*, 676-683.

Lehnert, B.P., Baker, A.E., Gaudry, Q., Chiang, A.S., and Wilson, R.I. (2013). Distinct roles of TRP channels in auditory transduction and amplification in *Drosophila*. Neuron *77*, 115-128.

Mazelova, J., Astuto-Gribble, L., Inoue, H., Tam, B.M., Schonteich, E., Prekeris, R., Moritz, O.L., Randazzo, P.A., and Deretic, D. (2009). Ciliary targeting motif VxPx directs assembly of a trafficking module through Arf4. EMBO J. *28*, 183-192.

Morthorst, S.K., Christensen, S.T., and Pedersen, L.B. (2018). Regulation of ciliary membrane protein trafficking and signalling by kinesin motor proteins. FEBS J. *285*, 4535-4564.

Park, J., Lee, J., Shim, J., Han, W., Lee, J., Bae, Y.C., Chung, Y.D., Kim, C.H., and Moon, S.J. (2013). dTULP, the *Drosophila melanogaster* homolog of tubby, regulates transient receptor potential channel localization in cilia. PLoS Genet. *9*, e1003814.

Patel, N.H. (1994). Imaging neuronal subsets and other cell types in whole-mount *Drosophila* embryos and larvae using antibody probes. In *Drosophila melanogaster*: Practical Uses in Cell and Molecular Biology, L.S.B. Goldstein and E.A. Fyrberg, eds. (London, UK: Academic Press), pp. 445-487.

Sharma, Y., Cheung, U., Larsen, E.W., and Eberl, D.F. (2002). pPTGAL, a convenient Gal4 P-element vector for testing expression of enhancer fragments in *Drosophila*. Genesis *34*, 115-118.

Sung, C.H. and Leroux, M.R. (2013). The roles of evolutionarily conserved functional modules in cilia-related trafficking. Nat. Cell Biol. *15*, 1387-1397.

Taschner, M. and Lorentzen, E. (2016). The intraflagellar transport machinery. Cold Spring Harb. Perspect. Biol. *8*, a028092.

Venken, K.J., He, Y., Hoskins, R.A., and Bellen, H.J. (2006). P[acman]: a BAC transgenic platform for targeted insertion of large DNA fragments in *D. melanogaster*. Science *314*, 1747-1751.

Walker, R.G., Willingham, A.T., and Zuker, C.S. (2000). A *Drosophila* mechanosensory transduction channel. Science *287*, 2229-2234.

Waters, A.M. and Beales, P.L. (2011). Ciliopathies: an expanding disease spectrum. Pediatr. Nephrol. *26*, 1039-1056.

Wright, K.J., Baye, L.M., Olivier-Mason, A., Mukhopadhyay, S., Sang, L., Kwong, M., Wang, W., Pretorius, P.R., Sheffield, V.C., Sengupta, P., et al. (2011). An ARL3-UNC119-RP2 GTPase cycle targets myristoylated NPHP3 to the primary cilium. Genes Dev. *25*, 2347-2360.

Yan, Z., Zhang, W., He, Y., Gorczyca, D., Xiang, Y., Cheng, L.E., Meltzer, S., Jan, L.Y., and Jan, Y.N. (2012). *Drosophila* NOMPC is a mechanotransduction channel subunit for gentle-touch sensation. Nature *493*, 221-225.